RSC Advances

ROYAL SOCIETY OF CHEMISTRY

www.rsc.org/advances

RSC Advances

ARTICLE

Evaluating effective factors on activity and loading of immobilized α-amylase onto magnetic nanoparticles using response surface-desirability approach

F. Eslamipour,[a] P. Hejazi[b*]

The effects of different operational conditions of α-amylase covalent immobilization on magnetic nanoparticles (MNPs), such as initial enzyme concentration, glutaraldehyde (GA) concentration, pH, ionic strength, were investigated using central composite design (CCD). Moreover, the two responses of biocatalyst activity and amount of immobilized enzyme were simultaneously studied by using Derringer's desirability function. The optimum amount and activity of immobilized enzyme were determined as 24.83% and 556.41 mg/g_{MNP} at 999.86 ppm initial enzyme concentration, solution pH of 4.6, 0.59% GA concentration, 99.99 mM ionic strength and 4 h process time. The study of kinetic parameters and enzyme stability showed significant enhancement in the performance of the immobilized enzyme with respect to the free enzyme. The storage stability and reusability of immobilized biocatalyst were obtained about 50 and 40% of the initial activity after 12 days and 6 cycle uses, respectively.

Received 00th January 20xx,
Accepted 00th January 20xx

DOI: 10.1039/x0xx00000x

www.rsc.org/

1. Introduction

The enzyme immobilization is one of the advantageous methods that improve the operation of biocatalysts in industrial bioprocess. It facilitates the enzyme separation from the reaction medium for recycling, stabilization in extreme conditions such as high pH or temperature, protection of enzymes against denaturing agents that can destroy the active site, increases life-time and thereby reduces the operating costs.[1]

Amylases are one of the most considerable hydrolase enzymes that occupied near the 30% of global enzyme market.[2] α-amylase (EC.3.2.1.1) is one of the amylase family which catalyzes the hydrolysis of internal α-1,4 glycosidic bonds in starch molecules and similar carbohydrates to maltose, glucose and other low molecular weight products.[3-5] The α-amylase has variety of applications such as starch saccharification, food, baking, fermentation, detergents, textiles and paper industry.[6] Owing to the wide industrial applications, the immobilization of α-amylase is a vital step to overcome the problems of using the free enzyme. The properties of immobilized biocatalyst are considerably depends on immobilization method and its conditions. There are many reports on the covalent immobilization of α-amylase on different supports, illustrating the advantages of immobilized enzyme such as increasing rigidity, retaining the enzyme activity, leakage and unfolding prevention during catalytic process.[1, 5, 7]

It should be noted that in former studies, limited number of factors such as enzyme concentration, time and pH were investigated for optimization of α-amylase[2, 4, 7, 8] So, despite the various conducted research on covalent α-amylase immobilization, there is a vacancy for a detailed investigation on different immobilization conditions and their interaction effects on the resulted biocatalyst efficiency. Moreover, optimization of different operating conditions with analyzing interactions between the effective factors on the activity and the amount of immobilized enzyme simultaneously could be very important for optimized biocatalyst development.[3, 4, 7] In our recent work, the effects of various immobilization conditions on covalent bond formation were investigated for α-amylase immobilization on magnetic nanoparticles (MNP).[7] However, it is vital to determine optimum immobilization conditions leading to perfect biocatalyst.

Response surface methodology (RSM) is recommended for multivariate studies because of its ability to produce empirical models and analysis the response of problems including several process factors by the approach of the response optimization. It is a collection of mathematical and statistical techniques which has been widely applied to optimize and evaluate interactive effects of independent variables in numerous enzymatic processes.[6, 9-11]

Multi-response surface method is used for solving the optimization problem of several responses. This methodology is applied when various responses have to be considered at the same time and there is a necessity for finding optimal

[a,b] Biotechnology Research Laboratory, School of Chemical Engineering, Iran University of Science and Technology, P.O. Box: 16846-13114, Tehran, Iran
†Electronic Supplementary Information (ESI) available: See DOI: 10.1039/x0xx00000x

compromises between the total numbers of responses taken into account.[12]

In this study, the multi-criteria decision making approach, Derringer's desirability function was used for the evaluation of two different responses (amount of immobilized enzyme and its activity). Applications and advantages of desirability functions have already been discussed in different informative articles.[13] To the best knowledge of the authors, there are no works to optimize the amount of enzyme loading and activity simultaneously with RSM and desirability functions.

For this, the covalent immobilization conditions of α-amylase on the magnetic nanoparticles were studied in detail by central composite design (CCD) under response surface methodology (RSM). Aminated magnetic nanoparticles activated by glutaraldehyde (GA) were used as support for immobilization. Different factors (initial enzyme concentration, GA concentration, pH, ionic strength and immobilization time) and their interactions were investigated simultaneously on the amount and activity of immobilized enzyme using statistical approach of RSM and multi-response optimization was done using Derringer's desirability function. The main and interaction of effective factors and the different importance values of both responses were analyzed. Also, different stabilities of α-amylase, reusability of biocatalyst and the kinetic factors of the immobilized and free enzyme were studied in the optimum condition.

2. Materials and methods

2.1. Materials

All chemicals, buffers and other reagents had analytical grade, and were used without further purification. Ferrous chloride ($FeCl_2 \cdot 4H_2O$) and ferric chloride ($FeCl_3.6H_2O$) were used as iron source. Aqueous ammonia (25% (v/v) aqueous solution) and ethanol were used as precipitation agent and solvent, respectively. All of these chemical were purchased from Merck. Crude α-amylase from Aspergillus oryzae (EC 3.2.1.15, activity 35.7 U/mg), GA, maltose, starch and 3,5 dinitro-salicylic acid (DNS) were purchased from Sigma–Aldrich. Deionized water (DI-water) was used in the preparation of all solutions.

2.2. MNPs synthesis and coating

The synthesis procedure and surface treatment of MNPs were reported in our previous work.[7] First, MNPs were synthesized by co-precipitation method and were covered by amino-silane functional groups via the silanization reaction using the 3-aminopropyltriethoxysilane (APTES). After that, aminated MNPs were activated with different amount of GA (0.5 and 10%) in 20 mM phosphate-citrate buffer (pH 7) according to the design of experiments.

2.3. Enzyme immobilization

Two milliliters of enzyme solution (250-1000 ppm) was added to 2 mg of MNPs as synthesized support which was equilibrated with 5-100 mM of phosphate-citrate buffer (pH 4.6-7.6). Thereafter, the mixture was shaken with the rotation speed of 200 rpm at 30 °C for different time periods (1-4 h) according to the design of experiments. All the experiments were done in triplicate and the mean value are reported as results. The amount of immobilized α-amylase on the support was determined using the Bradford`s method.[14]

2.4. Analysis methods and MNPs Characterization

2.4.1. Amylase activity assay

The activities of free and immobilized α-amylase were determined using the method proposed by Miller.[15] The number of reduced maltose molecules which produced in hydrolysis reaction of starch were measured with 3,5-dinitrosalicyli acid (DNS). The amount of produced maltose was determined using the UV spectroscopy at the wavelength 540 nm. amylase activity is defined as micromoles of maltose produced within 1 min at 30 °C.

2.4.2. Characterization of MNPs

The surface chemical groups were identified with Fourier transform infrared spectroscopy (FT-IR). The FT-IR spectra were recorded by Nicolet NEXUS 670 instrument. The Philips PW1800 diffractometer with Cu-Kα radiation (0.154056 nm) was used for X-ray diffraction (XRD) of nanoparticles. The morphology and particle size distribution of support material and biocatalyst were determined using transmission electron microscopy (TEM) and field emission scanning electron microscopy (FESEM). TEM imaging of MNPs was carried out with a Philips-CM30 microscope and FESEM micrographs were recorded using Philips-XL20.

2.5. Experimental design and statistical analysis

Preliminary experiments were carried out to determine the effective factors on the amylase immobilization process (data not presented here). A full factorial design was carried out to evaluating the effects of five important variables in two levels including initial enzyme concentration (250-1000 ppm), GA concentration (0.5-10 %), pH (4.6-7.6), ionic strength (5-100 mM) and immobilization time (1-4 h) on two responses of the amount of immobilized enzyme and its activity. Experimental design and analysis was done using 'Design Expert' software (version 8.0). A design of 36 experiments including, 32 trials of full factorial designs (2^5) and four replicates at the central points were used for the full factorial model. All tests were done in duplicate and the analysis of variance was performed based on these duplicate results. After ensuring that the curvature is important in the results of full factorial design, the levels of the immobilization factors and the interaction effects were analyzed and optimized by central composite design (CCD) of response surface methodology (RSM). For this purpose, 10 trials of face points were added to full factorial experimental design for converting it to RSM with α=1 (Table 1). A series of experiment at given optimal conditions were performed in order to study the validation of the response

surface model and compare the predicted values and experimental data.

2.6. Stability Tests

2.6.1. Thermal and pH stability

The thermal stability of immobilized enzyme using the optimum condition and free enzyme was studied in the temperature range of 30–80 °C. For this purpose, residual activities of the enzymes were measured after 30 min incubation in phosphate-citrate buffer (20 mM, pH=6) at each temperature.

The pH stability was investigated by evaluating the residual activity of enzyme after 30 min incubation of it at the certain pH in the range of 4–8 and at 30°C.

2.6.2. Storage stability and reusability

The storage stability of free and optimum immobilized α-amylase was investigated by measuring the residual activity (calculated as percentage of the initial activity) of them at different times (1-12 days). In addition, reusability of immobilized enzyme was evaluated by six cycle's activity test. The immobilized α-amylase was added to 2 ml of 1% (w/w) starch in 20 mM phosphate-citrate buffer (pH = 6) and incubated for 5 min under constant shaking speed at 30°C. The amounts of the immobilized enzymes that may be released during activity test were measured in each cycle via Bradford method. DNS method was used for measuring relative activity of residual immobilized enzyme in each cycle. After each cycle, the immobilized enzyme which was settled down using a strong magnet, washed with distilled water and then used for the next cycle.

2.7. Kinetic parameters

The activity of optimum immobilized and free enzyme was measured in different substrate concentrations (0.1–0.5 mg/ml). The K_m and V_{max} values were calculated from Lineweaver and Burk plot by using the in Michaelis-Menten model:

$$V^{-1} = \left\{\frac{K_m}{V_{max}}\right\}[S]^{-1} + V_{max}^{-1} \quad (1)$$

where [S] was the concentration of substrate and K_m was the Michaelis constant. V and V_{max} represented the initial and maximum rate of reaction, respectively.

3. Results and discussion

3.1. MNPs Characterization

The FTIR spectra of aminated MNPs (a), activated by GA (b) and immobilized α-amylase (c) are shown as Fig. 1. The peak observed at 1630 cm^{-1} corresponds to the bending mode of NH_2. The peak observed at 3438 cm^{-1} confirms the presence of N–H bond.[16, 17] The Fe–O bonding of activated magnetic nanoparticles can be indicated by two overlapped peaks at 590 and 610 cm^{-1}.[17] These peaks disappearance after enzyme immobilization (Fig.1-c), confirming full surface coverage of activated MNPs by amylase. Also, the broad peak around 1112 cm^{-1} indicates surface coverage by α-amylase after immobilization. The absence of characteristic peaks of GA and MNPs in Fig. 1-c suggests covalent bonding of GA and amylase[7].

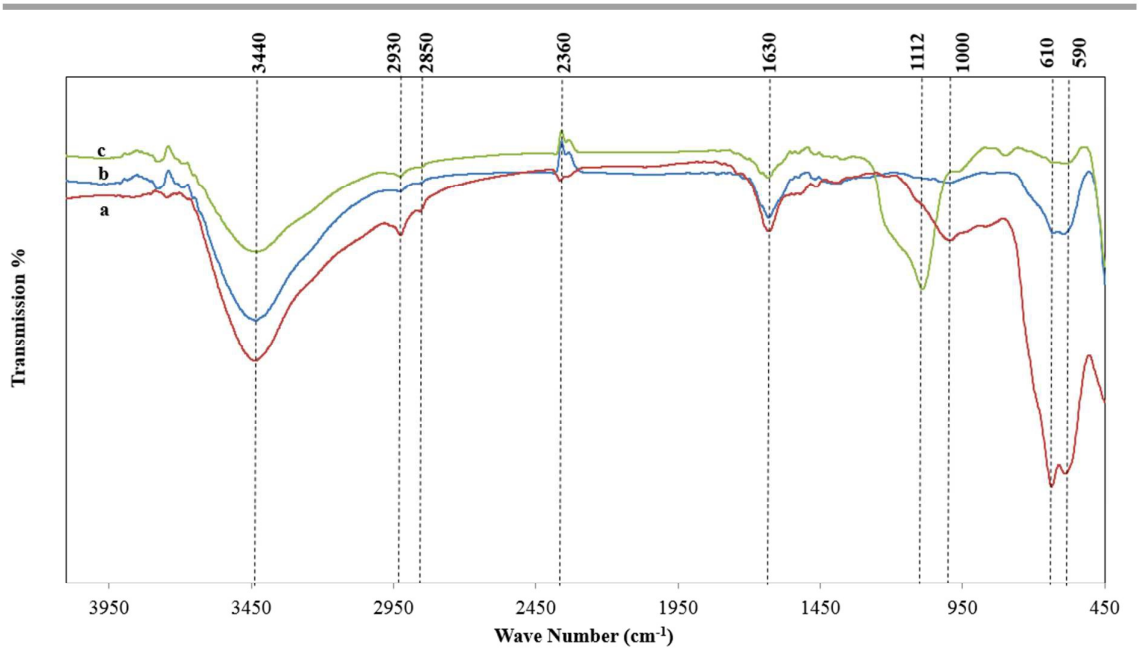

Fig. 1 FT-IR of bare MNP (a), GA activated MNP (b) and immobilized α-amylase on MNP (c).

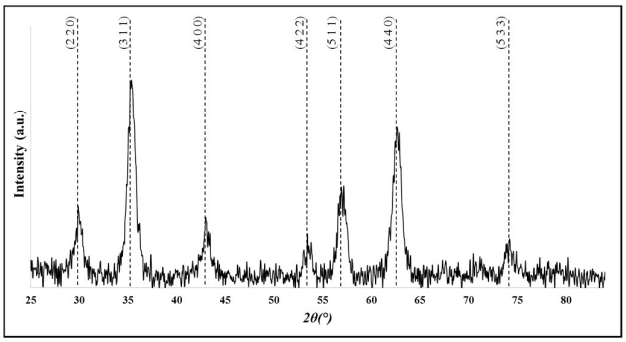

Fig 2 X-ray patterns of modified MNPs

Figure 2 shows the XRD pattern of modified MNPs with the corresponding diffraction planes. The characteristic diffraction peaks are assigned according to the reference pattern of JCPDS 01-087-0246. The crystalline structure of as-prepared magnetic nanoparticles is cubic. In addition, the sharp diffraction peaks confirms the perfect crystallinity of particles with an average crystallite size of 11.8 nm calculated with Scherrer equation. Prefect matching of diffraction peaks with the reference pattern demonstrates the phase purity of MNPs after surface modification.

Figure 3 shows the TEM micrograph and particle size distribution histogram of MNPs before and after immobilization. It demonstrates a narrow size distribution and uniform shape of MNPs. As shown in Fig. 3-a, before enzyme immobilization most of the particles have a size in range of 12 to 20 nm; the particles size distribution graph has a maximum in 15 nm. After enzyme loading on MNPs, the particle size increment was observed; as shown in Fig. 3-b, the maximum of particle size histogram was shifted from 15 to 20 nm. This particles size increment could be attributed to linker overlay and also immobilized enzyme on MNPs.

Fig. 4 shows the SEM images of the modified MNPs before and after enzyme immobilization. Fig. 4-a indicates uniform spherical particles; however, SEM images in Fig. 4 demonstrate the particles agglomeration with an average size of 50 nm compared to Fig. 3, which could be due to the presence of surface hydroxyl and amine groups, as demonstrated by FT-IR results. After immobilization (Fig. 4-b), the shape of amylase covered MNPs remained constant, whereas the average size of agglomerated particles increases to 70 nm.

3.2. Statistical analysis of experimental designs

Studying all of the effective factors and their interactions is necessary to optimize the immobilization process. The factors include initial enzyme concentration (C_{enz}), GA concentration (C_{GA}), pH, ionic strength (C_{buffer}) and time.

Two steps of experiments were designed to facilitate optimizing the α-amylase immobilization process. At first, the full factorial design with 32 experiments (the first 32 experiments in Table 1) and 4 experiments in center points levels (the last four experiments in Table 1) was used for studying the effects of five factors on the amount and activity of immobilized enzyme.

After confirming that the curvature is important in the ANOVA results of immobilized α-amylase activity in full factorial design (results not presented here), 10 experiments related to axial points of CCD were added to full factorial experimental design (experiment number 33-42 in Table 1). The levels of the immobilization factors and the results representing amount and activity of immobilized enzyme were obtained (Table 1) and the main and interaction effects were analyzed and optimized (Tables 1-S and 2-S in supplementary information) based on central composite design (CCD).

The second order mathematical equation as a result of 46 tests combination including regression coefficient (β) was obtained via the least square method. The model was evaluated by ANOVA for amount of immobilized enzyme and its activity depicted in Tables 1-S and 2-S, respectively.

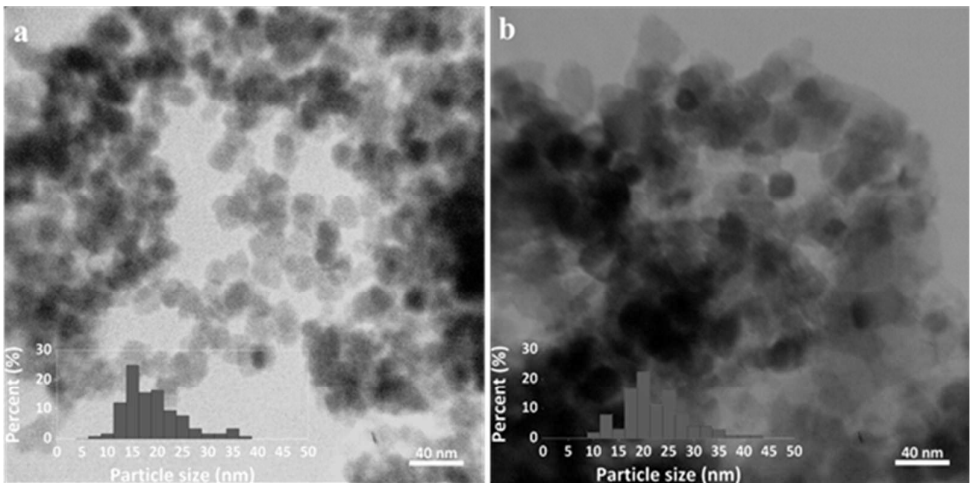

Fig 3 TEM images and particle size distribution histograms of MNPs before (a) and after (b) immobilization

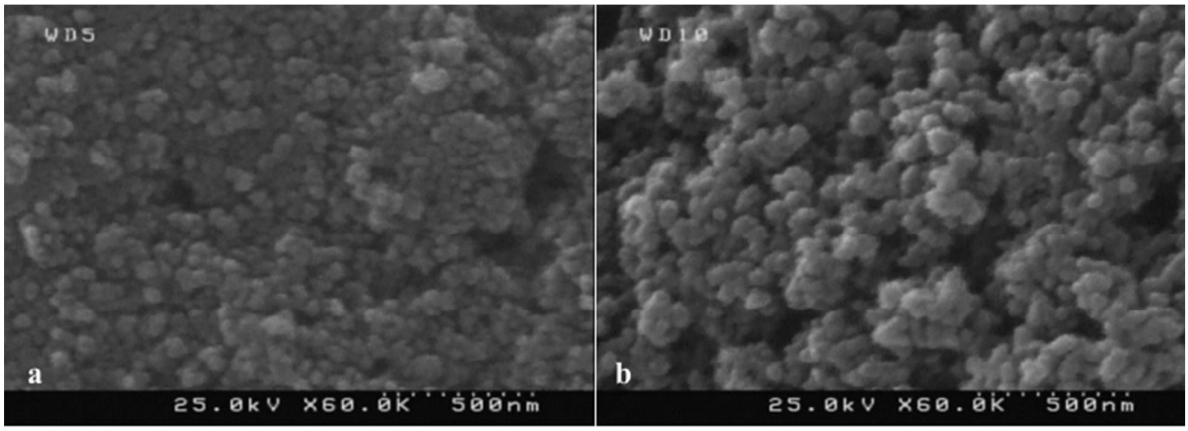

Fig. 4 SEM images of MNPs before (a) and after (b) immobilization

The variance analysis of quadratic regression model and low probability value of Fischer's F-test (<0.0001), indicate high significance of applied model. The F-values of 29.06 and 545.91 demonstrated that independent factors and their interactions had a significant effect on the activity and the amount of immobilized enzyme, respectively. The fitness of the model was investigated by determination coefficient (R-squared). In this case, the value of determination coefficients, 0.8713 for activity and 0.9958 for amount of immobilized enzyme, indicate that 12 and 1% of the total coefficients could not be determined by this model, respectively. In addition to, the high values of adjusted determination coefficients (Adj R-squared) represent the great significance of the model. The "Pre R-squared" was close to the "Adj R-squared".

The F-values of "Lack of Fit" of 1.56 and 0.0736 for activity and amount of immobilized enzyme respectively suggest the less significance relative to the pure error. In addition to Lack of Fit tests, the model was further evaluated by the observed vs. predicted plot. The points of all predicted and actual responses fell in 45° lines also indicate good agree with the model (results not presented here).

3.3. Effect of various factors on enzyme immobilization

3.3.1. Enzyme and GA concentrations

According to the main effects plots (not presented), the enzyme and GA concentrations have positive effects on the activity of immobilized enzyme. Fig. 5-(a,b) shows the 3D surface plot of GA and enzyme concentrations effects on the amount of immobilized enzyme and its activity. As shown in Fig. 5-(a,b), the amount and activity of immobilized enzyme increase by initial enzyme concentration in all GA concentration levels, but the activity increment rate is higher in the case of low concentrations of GA in comparison to high GA concentration.

In the other words, higher level of GA concentration resulted in lower activity when initial enzyme concentration increases (Fig. 5-a). Fig. 5-b demonstrates that immobilized enzyme loading increases by GA concentration until center point, then descends.

The increase of proper linkage sites via GA concentration increment, results in activity and enzyme immobilization increment. Then concentrating of GA in surface of MNPs leads to formation of GA dimmer molecules and decrease of linkage sites availability.[18] This phenomenon results in lower enzyme loading on MNPs, however higher mobility of enzyme bonded to GA leads to higher activity.[7, 19] Also, low concentration of enzyme, increases the possibility of single-point covalent bond formation leading to lower enzyme denaturation. [19]

In high enzyme concentration, GA concentration increment decreases the activity of biocatalyst. According to Nwagu and coworkers,[8] crosslinking between the enzymes via GA molecules leads to higher rigidity of enzyme and hence, lower activity. In addition, the high concentration of GA could change the globular structure of enzyme during immobilization process and therefore change its activity.[20]

3.3.2. Enzyme concentration and time

Fig. 5-(c,d) shows the effects of immobilization time on enzyme activity and loading. In different initial enzyme concentrations, the immobilized enzyme activity increase with the immobilization time increment (Fig. 5-c). Fig. 5-d illustrates that the immobilization time has no significant impact on the amount of immobilized enzyme.

It can be concluded from Fig. 5-c, that biocatalyst activity in higher process times is more affected by enzyme concentration in comparison to lower times. It has been reported that low concentration of enzyme during immobilization process increases the possibility of bonding between enzyme active site and linker leading to lower activity of biocatalyst. Moreover, it is possible to form multiple bonds between GA molecules and one enzyme. This means a decrease in activity of enzyme through rigidity increment.[8] In addition, increment of immobilization process time could increase the active site blockage possibility.

Fig. 5-(c,d) demonstrates increasing enzyme loading on support does not have the same increment on biocatalyst activity. This shows that immobilization time increment simultaneously

increases enzyme loading and active site blockage. Therefore, activity enhancement is not as significant as enzyme loading.

3.3.3. GA concentration and time

According to Fig. 5-e, in short-time experiment, immobilized biocatalyst activity increases with GA concentration. But in long-time experiment (4 hours), the activity falls down. In both levels of time, the amount of immobilized enzyme increases at first with increasing GA concentration, and then decays (Fig. 5-f). This behavior is corresponded to immobilization mechanism change from ionic adsorption to covalent bonding by GA concentration increment.[7]

The ascending activity rate of biocatalyst by GA concentration in short immobilization times can be attributed to enzyme loading. Fig. 5-f shows a maximum for enzyme loading around central points. Despite enzyme loading descending after central point, the activity increment of biocatalyst was observed (Fig. 5-e). This inconsistency could be corresponded to linker elongation via increasing GA concentration. This leads to higher mobility and reduced steric hindrance of anchored enzyme.[7, 19]

The biocatalyst activity meets a minimum around central point. The falling rate can be attributed to bonding increment between linker and enzyme, leading to higher rigidity. Decreasing the enzyme loading enhances biocatalyst activity via mobility enhancement.[8, 21]

Table 1 CCD of experiments and the results of amount and activity of immobilized α-amylase

Trial	C_{enz} (ppm)	C_{GA} (%)	Time (h)	pH	C_{buffer} (mM)	Immob. (mg/g_{MNP})	Act. (%)
1	250	0.5	1	4.6	5	76.46	0.50
2	1000	0.5	1	4.6	5	517.18	7.85
3	250	10	1	4.6	5	82.15	12.07
4	1000	10	1	4.6	5	591.51	11.86
5	250	0.5	4	4.6	5	75.09	10.69
6	1000	0.5	4	4.6	5	551.55	16.53
7	250	10	4	4.6	5	140.79	12.48
8	1000	10	4	4.6	5	667.34	17.89
9	250	0.5	1	7.6	5	81.96	0.43
10	1000	0.5	1	7.6	5	511.68	6.67
11	250	10	1	7.6	5	13.39	11.99
12	1000	10	1	7.6	5	466.13	13.80
13	250	0.5	4	7.6	5	88.83	11.79
14	1000	0.5	4	7.6	5	540.55	15.27
15	250	10	4	7.6	5	104.39	13.52
16	1000	10	4	7.6	5	593.53	18.17
17	250	0.5	1	4.6	100	101.20	1.50
18	1000	0.5	1	4.6	100	536.43	18.58
19	250	10	1	4.6	100	73.05	10.75
20	1000	10	1	4.6	100	607.68	12.07
21	250	0.5	4	4.6	100	89.52	8.88
22	1000	0.5	4	4.6	100	551.55	13.29
23	250	10	4	4.6	100	123.61	13.66
24	1000	10	4	4.6	100	656.22	16.93
25	250	0.5	1	7.6	100	79.21	0.00
26	1000	0.5	1	7.6	100	517.18	8.48
27	250	10	1	7.6	100	20.48	11.37
28	1000	10	1	7.6	100	465.12	10.89
29	250	0.5	4	7.6	100	86.21	5.80
30	1000	0.5	4	7.6	100	533.68	23.10
31	250	10	4	7.6	100	77.09	11.51
32	1000	10	4	7.6	100	523.76	17.27
33	250	5.25	2.5	6.1	52.5	134.48	7.46
34	1000	5.25	2.5	6.1	52.5	574.82	9.11
35	625	0.5	2.5	6.1	52.5	240.52	9.71
36	625	10	2.5	6.1	52.5	242.9	9.08
37	625	5.25	1	6.1	52.5	281.21	8.69
38	625	5.25	4	6.1	52.5	340.8	6.47
39	625	5.25	2.5	4.6	52.5	340.172	7.74
40	625	5.25	2.5	7.6	52.5	291.55	10.42
41	625	5.25	2.5	6.1	5	373.62	8.09
42	625	5.25	2.5	6.1	100	389.13	9.47
43	625	5.25	2.5	6.1	52.5	308.52	6.38
44	625	5.25	2.5	6.1	52.5	301.44	7.14
45	625	5.25	2.5	6.1	52.5	312.56	8.18
46	625	5.25	2.5	6.1	52.5	321.66	6.45

3.3.4. pH and ionic strength

According to ANOVA (Tables 1-S and 2-S), pH and ionic strength of immobilization medium were not efficient factors on biocatalyst activity and enzyme loading, respectively. The interaction plots are shown in Fig. 5-(g,h). As shown in Fig. 5-g, while the initial concentration of enzyme is low, high ionic strength solutions result in lower activity in comparison to low ionic strength solutions. The immobilizing mechanism of enzyme on GA activated support affects the activity of biocatalyst; since ionic strength of solution is one of the important determining factors on bonding type, it is an effective factor on activity.[22]

Physical bond formation is more favorable than covalent bonding in low ionic strength solutions and high number of reactive groups; so, in low ionic strength solutions immobilization initiates via physical adsorption and then continues with covalent bond formation. But in high ionic strength, covalent bond is the primary mechanism of immobilization.[7] So, when the initial concentration of enzyme is low, high ionic strengths results in covalent bond formation; therefore in this case biocatalyst shows lower activity in comparison to low ionic strength condition. But in high enzyme concentration, the high number of reactive amino acid groups leads to more physical bonds formation and results in higher activity.[22]

Fig. 5-h depicts that low pH of immobilization medium leads to higher enzyme loading. This behavior can be attributed to surface charge of support and enzyme. According to manufacturer data sheet, isoelectric point of α-amylase is 5.4. This indicates that surface charge of enzyme in high level pH is negative and in low level is positive. Also, negative surface charge of activated support was observed in both high and low level pHs via zeta potential measurement[7]. The surface charge data predicts that low pH immobilization media increases the enzyme loading via ion-ion interactions, also higher pH than 5.4 will retard immobilization rate via electrostatic hindrance [23]. Fig. 5-h depicts the pH effect on enzyme loading, these results is along with surface charge data and confirms enhancing effect of low pH immobilization environment.[4]

3.4. Optimization via the desirability function

In numerical optimization, the desired goal should be selected for each factor and response from the menu. The possible goals should be: maximize, minimize, target, within range, none (for responses only) and set to an exact value (factors only). Minimum and maximum levels must be imported for each factor included. Weights can be assigned to different goals to adjust the shape of its particular desirability function. The goals are combined into an overall desirability function. Desirability is an objective function that ranges from zero

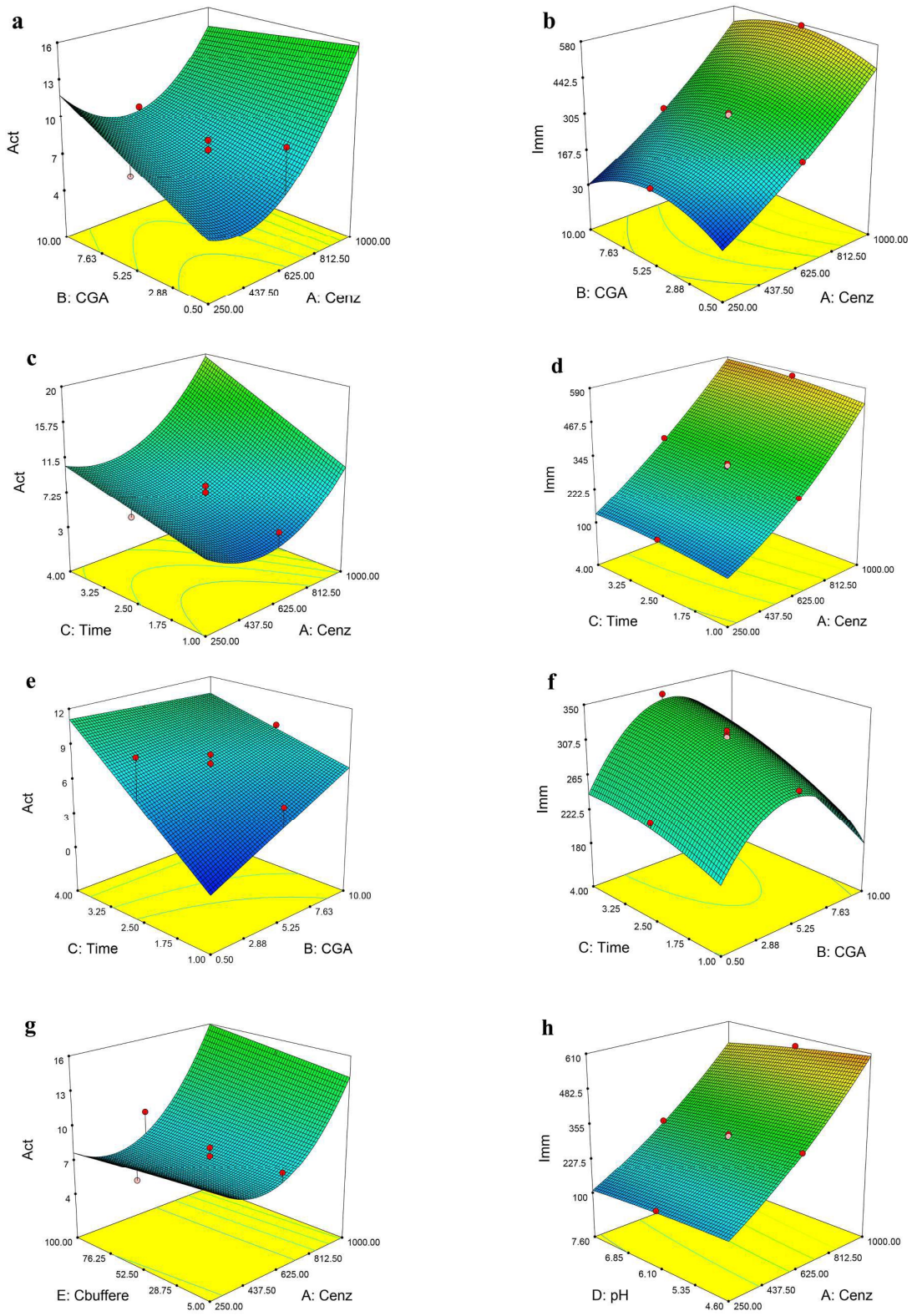

Fig. 5 Response surface plots representing interaction of enzyme and GA concentration (a,b), enzyme concentration and time (c,d), GA concentration and time (e,f), enzyme concentration and ionic strength (g), and enzyme concentration and pH (h) on activity and amount of immobilized enzyme respectively.

outside of the limits, to one at the goal which is maximized by program.[24]

Due to the curvature in the response surfaces and their combination in the desirability function, existence of more than two maximums is possible. Starting from several points in the design space increases the possibility of the best local maximum finding.[12, 25]

In this method, first each response (y_i) converts to an individual desirability function (d_i), and then the individual desirabilities are combined to give the overall desirability (D). The overall desirability function D is defined as the weighted geometric average of the individual desirability (d_f) according to equation (Eq. (2).[12, 26]

$$D = \sqrt[n]{d_1(y_1) \times d_2(y_2) \times \ldots \times d_3(y_2)} \quad (2)$$

where n is the number of studied responses in the optimization process. A multiple response method was applied for optimization of any combination of five goals, namely initial enzyme concentration, GA concentration, immobilization time, solution ionic strength and pH.

The numerical optimization seeks to maximize the desirability function.[27-29] All of the effective factors were set for maximum desirability. The goal of immobilized enzyme loading and the activity of obtained biocatalyst could be chosen in different ways. The results of choosing different goals and values of importance for the amount and activity of immobilized enzyme are reported in Table 2.

As it has been discussed in section 3-3, the activity of immobilized enzyme does not increase necessarily by enzyme loading. Therefore, choices of the goal in case of biocatalyst activity and enzyme loading, also their importance values have a significant effect on the optimum condition. As the aim of this work is obtaining a high activity and stability biocatalyst, so the goal of activity during optimization should be maximized. Also, in practical point of view, the biocatalysts with higher catalyst loadings are desired. Accordingly the immobilized enzyme loading should be maximized as well; but with lower importance in comparison to activity. According to Table 2, the changes in the importance of enzyme activity, as it was expected only leads to GA concentration change. The increase of GA concentration results in higher immobilization, hence higher activity; however in some cases, GA concentration increment leads to crosslinking of immobilized enzymes and activity decay via enzyme rigidity. Considering the aim of immobilization process, to obtaining a biocatalyst with high activity and enzyme loading, the immobilization condition with activity importance value of 5 has been chosen as optimum point. 3D surface plot desirability of the combined effects of initial enzyme concentration and GA concentration for optimal activity of immobilized enzyme were shown in Fig. 6.

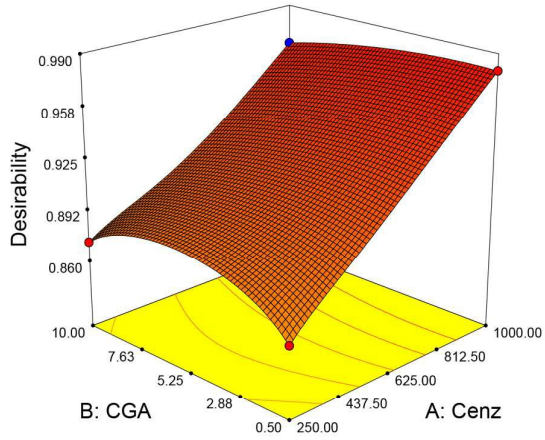

Fig. 6 Response surface plot of interaction of enzyme and GA concentrations and their effect on desirability.

The best local maximum was obtained at an initial solution pH 4.6, initial enzyme concentration 994.43, GA concentration of 0.59, time of 4 and ionic strength of 99.99. At these optimal conditions the enzyme immobilization and activity were measured to be 556.41 mg/g_{MNPs} and 24.83 % respectively at desirability value of 0.979. The value of obtained desirability shows that the D function represents the experimental model under desired conditions.

In order to verify the developed model, some of the experiments were carried out under optimum condition and the obtained data was compared with the predicted results from the model. The obtained experimental data for the optimum sample (activity=23.92%) showed acceptable fitness with model prediction (activity=24.8%), confirming model validity.

3.5. Results of Stability Tests

3.5.1. Thermal and pH stability

Fig. 7-a presents the relative activity of free and immobilized enzyme in the temperature range of 30-80 °C. The maximum

Table 2 Results of different numerical optimization conditions

Goal		Importance		Factor Level					Response		Desirability
Imm. (mg/gMNP)	Act. (%)	Imm. (mg/g_{MNP})	Act. (%)	C_{enz} (ppm)	C_{GA} (%)	Time (h)	pH	C_{buffer} (mM)	Imm. (mg/g_{MNP})	Act. (%)	
In range	Maximize	3	3	1000	0.50	3.9	5.7	100	554.84	23.99	0.930
Maximize	Maximize	3	3	1000	4.80	4	4.6	100	665.87	21.81	0.981
Maximize	Maximize	3	4	1000	1.61	3.8	4.6	99.89	595.12	23.84	0.979
Maximize	Maximize	3	5	994.43	0.59	4	4.6	99.99	556.41	24.83	0.979

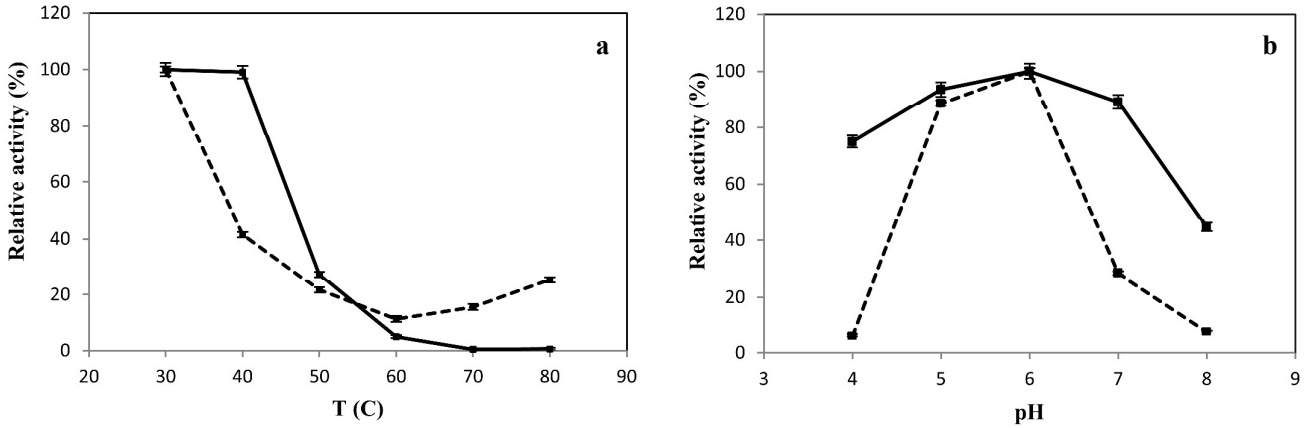

Fig. 7 Temperature (a) and pH (b) stabilities of the immobilized enzyme (solid line) and free (dash line).

activity for both free and immobilized enzymes were observed in 30°C. The relative activity loss by temperature increment (above 60°C) was approximately 80% for the immobilized enzyme and 100% for the free one. As it can be seen in the figure, the immobilized amylase was more stable than the free amylase.

The increase in stability could be the result of improvement in enzyme rigidity through covalent immobilization.[7, 30]

The effects of pH on the free and immobilized α-amylase were studied in the range of 4.0–8.0. As it can be seen in Fig. 7-b, the maximum activity of free and immobilized enzyme occurs at pH 6. According to the results, pH variations have less effect on immobilized enzyme activity in comparison to free enzyme. The figure shows that the activity of immobilized enzyme is higher than 80% in wide range of pH compared to the free; the higher stability of immobilized biocatalyst corresponds to conformational rigidity and the diffusional limitations of the immobilized molecules.[31]

3.5.2. Storage stability and reusability

The residual activity as a function of cycles was presented in Fig. 8-a. According to the results, the optimum biocatalyst kept near the 40% of its initial activity after six cycles. The immobilized enzyme was not released during the experiments, so the activity decline could be related to the conformational changes in the immobilized enzyme structure.[31]

Fig. 8-b illustrates the relative activity of immobilized and free α-amylase, stored in 20 Mm phosphate-citrate buffer (pH=7) at 4°C. The activity was measured for 12 days. The amounts of remained relative activity of immobilized and free enzyme were about 50 and 23% respectively after 12 days. It confirms that α-amylase becomes more stable via immobilization.

3.6. Kinetic parameters

The Lineweaver-Burk plot was generated using the results of free and immobilized enzyme (at optimal conditions) at pH=6 and 25°C (Fig. 1-S).

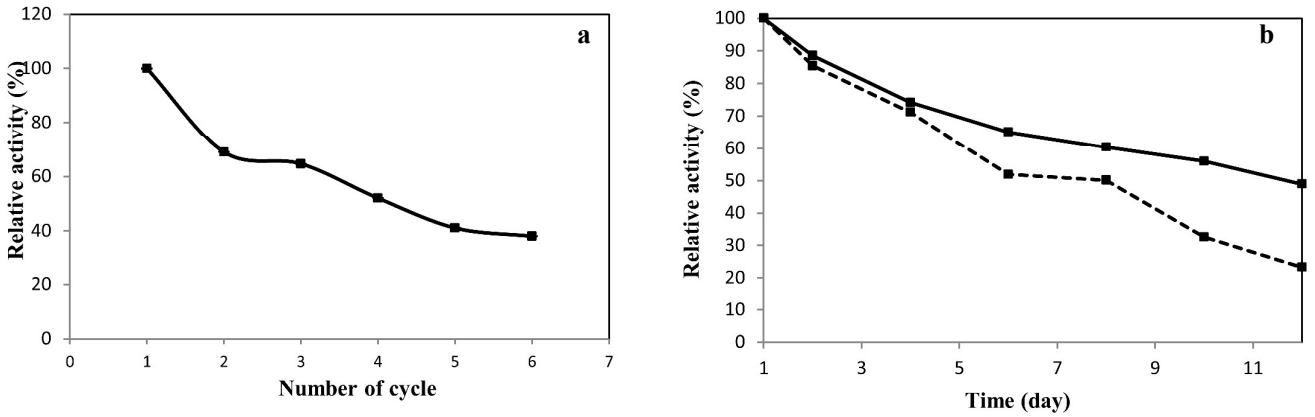

Fig. 8 Catalyst recycling of the immobilized enzyme (a), storage stability of the immobilized (solid line) and free (dash line) α-amylase (b).

Table 3 Optimized properties of immobilized α-amylase in the present and other studies

Carrier	Loading (mg/g)	Activity (%)	K_m				V_{max}				Ref
			Free		Immobilized		Free		Immobilized		
Gum acacia stabilized Fe_3O_4 MNPs	0.6	-	2.2	mg/ml	2.9	mg/ml	3.4	U/ml	5.3	U/ml	[1]
Silica coated Fe_3O_4 MNPs	11.5	19.6	5.0	mg/ml	2.5	mg/ml	0.21	U/mg	0.78	U/mg	[2]
Dye attached magnetic Fe3O bead	401	10.5	0.780	mg/ml	0.785	mg/ml	4.09	U/mg	5.98	U/mg	[4]
Silica coated Fe_3O_4MNPs	15	-	6.27	mM	4.77	mM	2.44	U/mg	11.58	U/mg	[5]
Modified Fe_3O_4 MNPs	556.41	24.8	0.092	mM	0.053	mM	7.96	U/mg	5.36	U/mg	This study

The K_m values for free and immobilized enzymes were calculated as 0.092 and 0.053 mM, respectively. The lower K_m values represent the higher affinity of the enzymes to substrates. According to the results, the affinity of α-amylase to its substrate was increased through immobilization. It could be attributed to the nonporous structure of MNPs that forces enzyme molecules to be expanded over the MNPs surfaces through proper orientation, leading to high available active sites[5] The values of V_{max} for free and immobilized enzymes were found as 7.96 and 5.36 μmol/(mg.min), respectively. Since enzymatic reactions have high reaction rates at enzyme active sites, the mass transfer of substrate to active site is the rate determining step in these reactions. Hence, the decline in V_{max} after immobilization corresponds to mass transfer limitation of the diffuse layer around the biocatalyst particle.[31]

Table 3 compares the result of current study with activity, enzyme loading, and biocatalytic kinetics of recent works regarding amylase immobilization on magnetic nanoparticles. A significant enzyme loading and activity enhancement are observed. This multiple fold enzyme loading increment could be corresponded to the optimization of effective factors in immobilization process; leading to immobilization of enzyme via different physical and covalent mechanisms. The multifunctional surface of support, containing high concentration of amino groups and activated by GA, increased considerably the amylase loading capacity of support. Also, remarkable decrease of K_m indicates affinity increment of α-amylase to the substrate.

4. Conclusions

Aiming at an optimum immobilization route of α-amylase on the MNPs, factors impacting immobilization process and their interactions were investigated using CCD. The initial enzyme concentration, solution pH, GA concentration, ionic strength and time significantly influenced the amount and activity of immobilized enzyme. These were optimized for maximum efficiency of immobilized enzyme by applying a desirability function. A dimensionless individual desirability value of 0.979 indicates the estimated function properly represents the experimental model under desired conditions. The optimum immobilized α-amylase demonstrates remarkable activity, enhancement of pH and temperature stabilities, as well as increasing reusability, storage time and substrate affinity.

References

1. V. Swarnalatha, R. A. Esther and R. Dhamodharan, Journal of Molecular Catalysis B: Enzymatic, 2013, 96, 6-13.
2. A. Mukherjee, T. Kumar, S. Rai and J. Roy, Biotechnology and Bioprocess Engineering, 2010, 15, 984-992.
3. M. J. Khan, Q. Husain, A. Azam, Biotechnology and Bioprocess Engineering, 2012, 17, 8.
4. N. Tüzmen, T. Kalburcu and A. Denizli, Journal of Molecular Catalysis B: Enzymatic, 2012, 78, 16-23.
5. N. Sohrabi, N. Rasouli, M. Torkzadeh, Chemical Engineering Journal 2014, 240, 426–433.
6. K. Singh and A. M. Kayastha, Journal of Molecular Catalysis B: Enzymatic, 2014, 104, 75-81.
7. F. Eslamipour and P. Hejazi, Journal of Molecular Catalysis B: Enzymatic, 2015, 119, 1-11.
8. T. N. Nwagu, B. Okolo, H. Aoyagi and S. Yoshida, Process Biochemistry, 2013, 48, 1031-1038.
9. S. J. Kalil, F. Maugeri and M. I. Rodrigues, Process Biochemistry, 2000, 35, 539-550.
10. M. Amini, H. Younesi, Clean - Soil, Air, Water, 2009, 37, 10.
11. S. A. Talat M, Srivastava ON., Bioprocess Biosystem Engineering, 2011, 34, 11.
12. M. A. Bezerra, R. E. Santelli, E. P. Oliveira, L. S. Villar and L. A. Escaleira, Talanta, 2008, 76, 965-977.
13. M. A. Islam, M. R. Alam and M. O. Hannan, Composites Part B: Engineering, 2012, 43, 861-868.
14. M. M. Bradford, Analytical Biochemistry, 1976, 72, 248-254.
15. G. L. Miller, Anal. Chem., 1959, 31, 426–428.
16. C. Guo, M. Yunhui, S. Pengfei, F. Baishan, Biochemical Engineering Journal 2012, 67, 120– 125.
17. K. Can, M. Ozmen, M. Ersoz, Colloids and Surfaces B: Biointerfaces 2009, 71, 154–159.
18. L. J. Liu H, Tan B., Zhou F., Qin Y., Yang R., Bioprocess Biosystem Engineering, 2012, 35, 8.
19. A. S. Campbell, C. Dong, F. Meng, J. Hardinger, G. Perhinschi, N. Wu and C. Z. Dinu, ACS Applied Materials & Interfaces, 2014, 6, 5393-5403.
20. Y. J. Cho, O. J. Park and H. J. Shin, Enzyme and Microbial Technology, 2006, 39, 108-113.
21. G. Bayramoğlu, S. Kiralp, M. Yilmaz, L. Toppare and M. Y. Arıca, Biochemical Engineering Journal, 2008, 38, 180-188.
22. O. Barbosa, C. Ortiz, A. Berenguer-Murcia, R. Torres, R. C. Rodrigues, R. Fernandez-Lafuente, RSC Advances, 2014, 4, 1583-1600.
23. S. Talekar, A. Joshi, G. Joshi, P. Kamat, R. Haripurkar and S. Kambale, RSC Advances, 2013, 3, 12485-12511.
24. H. Heidari and H. Razmi, Talanta, 2012, 99, 13-21.

25. M. Mourabet, A. E.l Rhilassi, H. El Boujaady, M. Bennani-Ziatni and A. Taitai, Arabian Journal of Chemistry, 2014, DOI: http://dx.doi.org/10.1016/j.arabjc.2013.12.028.
26. M. Fereidouni, A. Daneshi and H. Younesi, Journal of Hazardous Materials, 2009, 168, 1437-1448.
27. R. Singh, N. R. Bishnoi and A. Kirrolia, Bioresource Technology, 2013, 138, 222-234.
28. M. Mourabet, A. E.l Rhilassi, H. E.l Boujaady, M. Bennani-Ziatni, R. E.l Hamri and A. Taitai, Journal of Saudi Chemical Society, 2015, 19, 603-615.
29. R. Singh, N. R. Bishnoi, A. Kirrolia., Bioresource Technology, 2013, 138, 222-234.
30. A. Pal and F. Khanum, Process Biochemistry, 2011, 46, 1315-1322.
31. G. Srivastava, S. Roy and A. M. Kayastha, Food Chemistry, 2015, 172, 844-851.